

# Development of cryogenic phonon detectors based on $\text{CaMoO}_4$ and $\text{ZnWO}_4$ scintillating crystals for direct dark matter search experiments

I. Bavykina<sup>a,\*</sup> G. Angloher<sup>a</sup> D. Hauff<sup>a</sup> M. Kiefer<sup>a</sup> F. Petricca<sup>a</sup> F. Pröbst<sup>a</sup>

<sup>a</sup>*Max-Planck-Institut für Physik (Werner-Heisenberg-Institut), Föhringer Ring 6, 80805 Munich, Germany*

Received 6 June 2008; revised 23 September 2008; accepted 30 September 2008

---

## Abstract

This work reports on the development of the first phonon detectors based on  $\text{CaMoO}_4$  and  $\text{ZnWO}_4$  scintillating crystals for the CRESST-II experiment. In particular, a novel technique for the production of the  $\text{ZnWO}_4$  phonon detector with a separate thermometer carrier was investigated. The influence of the thermal and mechanical treatment on the scintillation light output of  $\text{CaMoO}_4$  and  $\text{ZnWO}_4$  crystals at room temperature is discussed.

*Key words:* Scintillation detectors, Dark Matter, Low temperature techniques,  $\text{CaMoO}_4$ ,  $\text{ZnWO}_4$

*PACS:* 29.40.Mc, 95.35.+d, 07.20.Mc

---

## 1. Introduction

The kinematics of galaxies and galaxy clusters suggests that the dynamic mass involved is far greater than the observable luminous mass [1]. The detection of hypothetical new particles constituting the missing mass of the Universe (the so-called Dark Matter) still remains one of the outstanding experimental efforts of present-day astrophysics and cosmology. In CRESST-II (second phase of the Cryogenic Rare Event Search with Superconducting Thermometers) direct dark matter search experiments we are looking for WIMPs (Weakly Interacting Massive Particles) [2]. These particles are supposed to be gravitationally bound in a non-rotating roughly isothermal halo around the visible part of our galaxy with a density of about  $0.3 \text{ GeV}/\text{cm}^3$  at the position of the Earth [3]. We expect interaction with ordinary matter via elastic scattering on target nuclei. In case of a spin-independent WIMP-nucleon scattering the interaction cross-section is proportional to  $A^2$  (where  $A$  is atomic mass), thus favoring heavy nuclei in the target.

The present CRESST-II experimental setup at the Laboratori Nazionali del Gran Sasso (LNGS, Italy) involves a 66 channel SQUID readout system to enable operation of

33 detector modules which can house up to 10 kg of the target material [4, 5].

## 2. Conventional CRESST-II detector module

The CRESST collaboration developed a reliable technique to produce sensitive cryogenic phonon detectors based on scintillating crystals [6]. When supplemented with a light detector these provide an efficient discrimination of nuclear recoils from radioactive  $\alpha$ -,  $\beta$ - and  $\gamma$ - backgrounds while simultaneously measuring phonon and light signals caused by particle interactions in the scintillating crystal [7, 8].

A conventional CRESST-II detector module consists of a cryogenic phonon detector based on a scintillating dielectric crystal and a nearby but separated light detector, optimized for the detection of scintillation light, see Figure 1.

Each detector has a tungsten superconducting phase-transition thermometer (W-SPT) evaporated onto the surface. The thermometer layout is described in [7]. We operate both detectors as cryogenic calorimeters detecting pulses on event by event basis while stabilizing the detectors within the superconducting-to-normal state of their transition curves. There a small temperature rise  $\Delta T$  of the W-SPT leads to a measurable rise  $\Delta R$  of its resistance, which can be read out with sensitive electronics. Since the

---

\* Corresponding author: tel: +49 89 323 54 316; fax: +49 89 323 54 526

*Email address:* bavykina@mppmu.mpg.de (I. Bavykina).



Fig. 1. An open CRESST-II detector module for coincident phonon and light measurements. On the left side: Silicon on sapphire light detector with W-SPT mounted in a copper holder. On the right side: Phonon detector based on a  $\text{CaWO}_4$  scintillating crystal with W-SPT mounted in a copper holder. The crystal is held by six pairs of bronze clamps coated with an Al layer and with an Araldite 2011 scintillating layer [11]. The whole structure is surrounded by highly reflecting foil (VM2002).

shape and the steepness of the transition curve determines the dynamical range and the linearity of the detector response function, steep and narrow transition curves with transition temperatures as low as 20 mK are desirable.

To improve the collection of the scintillation light the whole structure is surrounded by a highly reflecting scintillating foil (VM2002)<sup>1</sup>.

### 2.1. Phonon detectors

The copper housing is designed to hold scintillating crystals of cylindrical shape, 40 mm in diameter and 40 mm in height. All of our crystals (see Table 1) have small  $\sim 0.5$  mm bevels. All surfaces are mechanically polished with silk to optical quality (with accuracy better than  $\lambda$ ) except one flat surface which is roughened with 10  $\mu\text{m}$  grain size.

The absence of a noticeable degradation of the light yield for events near the crystal surface is essential for our crystals to be operated as phonon detectors at low temperatures [8]. Therefore, chemically stable and non-hygroscopic crystals are favored as scintillating targets. Since the crystals are thoroughly held by six pairs of metal clamps in the holder, it is important that they are mechanically stable.

In the CRESST-II experiment we use calcium tungstate crystals as target material [7]. Among different scintillators  $\text{CaWO}_4$  was selected because of its relatively high light yield at low temperature<sup>2</sup>. Due to the need of CRESST-II to further improve the capability of rejecting background caused by known particles scintillating crystals with a light yield higher than that of  $\text{CaWO}_4$  are constantly under in-

<sup>1</sup> VM2002 is a registered trademark of the 3M company. This foil has a sharp cutoff in reflectivity from  $\sim 99$  % to almost 0 % for wavelengths lower than  $\sim 390$  nm at room temperature.

<sup>2</sup> The light yield of the scintillating crystal at low temperatures determines the discrimination threshold between nuclear and electron recoils.

Table 1

Properties of  $\text{CaWO}_4$ ,  $\text{ZnWO}_4$  and  $\text{CaMoO}_4$  scintillating crystals. The data are taken from [10]; the light yield (LY) and scintillation decay time constant  $\tau_{scint}$  of  $\text{CaMoO}_4$  are taken from [9].

	$\text{CaWO}_4$	$\text{ZnWO}_4$	$\text{CaMoO}_4$
Crystal structure	scheelite	wolframite	scheelite
Cleavage (plain)	weak (101)	marked (010)	weak (001)
Index of refraction	1.93	2.10	1.98
Melting point ( $^\circ\text{C}$ )	$\sim 1650$	$\sim 1200$	$\sim 1430$
Density ( $\text{g}/\text{cm}^3$ )	6.1	7.8	4.5
Emission max at 300 K	420	480	520
Light Yield at 300 K (ph/MeV)	6000	21500	1720
$\tau_{scint}$ at 300 K ( $\mu\text{s}$ )	0.6	22	20
Debye frequency (THz)	$\sim 4.7$	$\sim 3.8$	$\sim 8.2$

vestigation. Additionally, for the interpretation of the positive WIMP signature, it is beneficial to have targets with a variety of nuclei.

### 2.2. Light detectors

The scintillating light signal is measured using a separate light detector made either from a sapphire wafer (40 mm in diameter and  $\sim 0.4$  mm thick) with an epitaxially grown silicon absorber layer, or made from a silicon wafer with a similar shape (40 mm in diameter and  $\sim 0.4$  mm thick) of square ( $30 \times 30 \times 0.45$ )  $\text{mm}^3$  shape [12].

## 3. Phonon detectors based on $\text{CaMoO}_4$ crystals

The comparison between the WIMP-nucleon interaction rate on different target materials would give us unique possibility to verify a positive WIMP signal and to learn about WIMP properties. For example, on a  $\text{CaMoO}_4$  target WIMPs are expected to scatter mainly on molybdenum nuclei<sup>3</sup> whereas on a  $\text{CaWO}_4$  or a  $\text{ZnWO}_4$  target they would mainly scatter on tungsten nuclei. Figure 2 shows the integrated recoil spectra plotted as a function of the discrimination threshold energy expected for 100  $\text{GeV}/c^2$  WIMPs scattering on various scintillating targets with a spin-independent WIMP-nucleon scattering cross-section of 1 pb [13]. The count rate on a  $\text{CaMoO}_4$  target above a discrimination threshold of  $\sim 14$  keV is higher than that on a  $\text{CaWO}_4$  target. In a  $\text{CaWO}_4$  target most of the WIMP induced recoils are expected to appear below 40 keV, while in a  $\text{CaMoO}_4$  target this value is shifted towards a higher energy of  $\sim 60$  keV.

<sup>3</sup> This is due to the factor  $A^2$  in the spin-independent scattering cross-section.

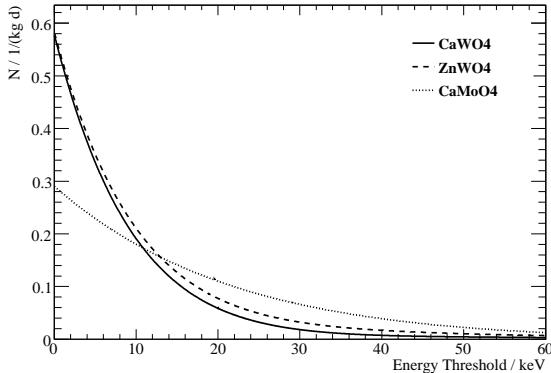


Fig. 2. The integrated recoil spectra expected for  $100 \text{ GeV}/c^2$  WIMPs scattered elastically on  $\text{CaWO}_4$  (solid line),  $\text{ZnWO}_4$  (dashed line) and  $\text{CaMoO}_4$  (dotted line) targets. Coherent WIMP-nucleon scattering cross-section is  $1 \text{ pb}$ . The used dark matter profile is described in Section 1.

The first characterization of the light yield of the  $\text{CaMoO}_4$  crystals at a temperature of  $8 \text{ K}$  proofed the potential of these scintillating crystals as target material. It was measured that the light yield increases progressively with decreasing temperature [14]. We are currently measuring the light yield of a  $\text{CaMoO}_4$  sample at mK temperatures in an assembly similar to the conventional CRESST-II detector module (see Section 2).

Last but not least,  $\text{CaMoO}_4$  is an excellent candidate to search for neutrinoless double- $\beta$  decay ( $0\nu 2\beta$ ) of  $^{100}\text{Mo}$  [15, 16]. The integration of phonon detectors based on  $\text{CaMoO}_4$  crystals into the CRESST-II experiment would give us the interesting possibility to perform a multi-experiment with only one target material and to obtain a competitive upper limit on the half-life of  $0\nu 2\beta$  decay of  $^{100}\text{Mo}$ .

### 3.1. Relative light yield of $\text{CaMoO}_4$ crystals at room temperature

Two cylindrically chopped ( $40 \text{ mm}$  in diameter and  $40 \text{ mm}$  in height) crystals considered in this work were produced by the Czochralsky technique at Bogoroditsk Plant of Technochemical Products (BTCP, Bogoroditsk, Tula region, Russia) from purified raw materials. The relative light yield (RLY) at room temperature was measured using a green extended PMT Photonis (XP3461B)<sup>4</sup> with a base modified to integrate scintillation light over  $400 \mu\text{s}$ . The crystals were mounted in a plastic holder of  $50 \text{ mm}$  in diameter. The wall of the holder was covered with a reflecting foil (VM2002). Crystals were measured without optical coupling to the PMT and were irradiated by  $662 \text{ keV}$   $\gamma$ 's from a  $^{137}\text{Cs}$  source. For each crystal the measured light yield with applied spectral correction [18] was normalized to the light yield of our standard  $\text{CaWO}_4$  crystal ( $=40 \text{ mm}$ , height= $40 \text{ mm}$ ). The results of the RLY measurements of

<sup>4</sup> The quantum efficiency of a Photonis XP3461B is maximal around  $420 \text{ nm}$ .

Table 2

Relative light yield of  $\text{CaMoO}_4$  crystals measured at room temperature with a PMT. The light yield of each  $\text{CaMoO}_4$  crystal with applied spectral correction was normalized to the light yield of our standard  $\text{CaWO}_4$  crystal (see text for details).

	RLY (%)	Resolution (%)
	at $662 \text{ keV}$	
$\text{CaMoO}_4$ -1 as arrived	17	33.7
$\text{CaMoO}_4$ -1 annealed	15.5	37.6
$\text{CaMoO}_4$ -1 with W-SPT, annealed, roughened	20.4	26
$\text{CaMoO}_4$ -2 with W-SPT, roughened, no annealing	22	23.7

$\text{CaMoO}_4$  crystals ( $=40 \text{ mm}$ , height= $40 \text{ mm}$ ) at room temperature are summarized in Table 2. The energy resolution was estimated as the FWHM divided by the position of the  $662 \text{ keV}$  line.

Since after-growth annealing at high temperatures can have a significant influence on the scintillation properties of the crystals we performed a series of tests to investigate this issue. Annealing at  $800 \text{ }^\circ\text{C}$  for 48 hours in oxygen flow<sup>5</sup> degraded the light yield and the energy resolution of the crystal  $\text{CaMoO}_4$ -1 to  $15.5 \%$  and to  $37.6 \%$ , respectively (see Fig. 3). Since smaller ( $20 \times 10 \times 5$ )  $\text{mm}^3$   $\text{CaMoO}_4$  samples were not annealed in oxygen flow by the producer they have shown an increase of the RLY after annealing performed at  $800 \text{ }^\circ\text{C}$  for 48 hours in oxygen flow.

Roughening of one of the flat crystal surfaces with boron carbide powder which followed W-SPT deposition (see Section 3.2) improved the light yield and the energy resolution to  $20.4 \%$  and  $26 \%$ , respectively. This increase was expected since more scintillating photons were able to escape through the roughened surface facing the PMT.

### 3.2. W-SPT on $\text{CaMoO}_4$ crystals

For the W-SPT deposition a crystal was mounted in a tantalum holder (which can be kept at the desired deposition temperature via radiative heating) into the tungsten deposition system. Before deposition an area below a thermometer on the  $\text{CaMoO}_4$  crystal surface was roughened on atomic level with an ion-gun. This procedure improves the adhesion of the film to the crystal surface. Before the deposition the crystal was slowly heated up to  $450 \text{ }^\circ\text{C}$  in vacuum and then kept at this temperature during the whole deposition process. To prevent inter-diffusion between the tungsten film and the  $\text{CaMoO}_4$  crystal surface we deposited  $2 \text{ k}$  layer of  $\text{SiO}_2$ . Then a  $2 \text{ k}$  layer of tungsten was evaporated. There was no crystal quality degradation observed after W-SPT deposition.

<sup>5</sup> It was not known at this time that the producer annealed the crystal  $\text{CaMoO}_4$ -1 at  $\sim 1300 \text{ }^\circ\text{C}$  in oxygen flow.

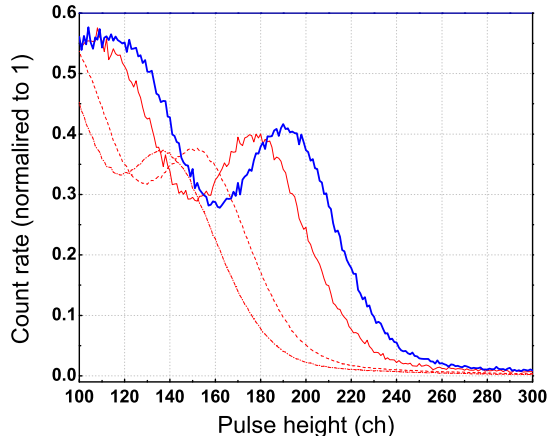


Fig. 3.  $^{137}\text{Cs}$  spectra measured with the  $\text{CaMoO}_4$ -1 crystal before annealing (dashed line), after annealing at  $800\text{ }^\circ\text{C}$  for 48 hours in oxygen flow (dash dotted line), and after W-SPT deposition with subsequent surface roughening (thin solid line), together with  $^{137}\text{Cs}$  spectrum measured with a different crystal  $\text{CaMoO}_4$ -2 after W-SPT deposition with subsequent surface roughening (thick solid line). Measurements were performed at room temperature with a PMT (see text for details).

The resistance of the thermometer was measured by passing a constant bias current through the readout circuit in which the thermometer was in parallel with a small shunt resistor and an input coil of a dc-SQUID. While cooling to the base temperature of a dilution fridge a decrease in the thermometer resistance was measured as a current decrease through the SQUID input coil (for details see [7]). The resistances between  $\sim 130\text{ m}\Omega$  and  $\sim 200\text{ m}\Omega$  of the W-SPT on the  $\text{CaMoO}_4$  crystals were measured as described above while applying  $1\text{ }\mu\text{A}$  bias current. Steep and narrow transition curves with transition temperatures of  $\sim 18\text{ mK}$  and width of a few mK were achieved, see Fig. 4. The characteristics of the obtained transition curves fulfill the quality requirements of the W-SPT for the CRESST-II phonon detectors.

The thermal response [19] of the W-SPT on the  $\text{CaMoO}_4$ -1 crystal which was stabilized in the normal-to-superconducting state has shown promising results. However, due to the high count rate on ground level ( $\sim 50\text{ Hz}$ ) no calibration spectrum was recorded.

#### 4. Phonon detectors based on $\text{ZnWO}_4$ crystals

In search of scintillators with high light yield at mK temperatures we also analyzed  $\text{ZnWO}_4$  crystals in detail. The results of the research have shown that the relative light yield of  $\text{ZnWO}_4$  at low temperatures is comparable with that of  $\text{CaWO}_4$  [21, 22]. Additionally, the count rate from  $\text{ZnWO}_4$  crystals due to internal radioactive impurities is expected to be lower than that from  $\text{CaWO}_4$  crystals [20]. Thus,  $\text{ZnWO}_4$  appears to be an attractive target for the CRESST-II dark matter search and the first proto-

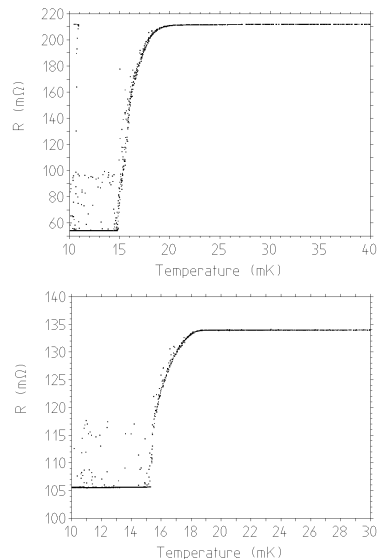


Fig. 4. The transition curves of W-SPT on the  $\text{CaMoO}_4$ -1 crystal (top) and of W-SPT on the different  $\text{CaMoO}_4$ -2 crystal (bottom) recorded with a  $1\text{ }\mu\text{A}$  bias current.

type phonon detector based on this material was developed.

##### 4.1. Relative light yield of $\text{ZnWO}_4$ crystals at room temperature

All  $\text{ZnWO}_4$  crystals considered in this work were produced by the unique low temperature gradient Czochralsky technique [23] at Nikolaev Institute of Inorganic Chemistry (NIIC, Novosibirsk, Russia). The results of the spectroscopic analysis of one of the  $\text{ZnWO}_4$  crystal measured with a high purity germanium detector in the Garching underground laboratory (Technische Universität München) are summarized in Table 3. Since the density of the crystal is rather high, the germanium detector efficiencies for small  $\gamma$  energies are rather low, thus leading to higher upper limits for the activities.

The relative light yield of the crystals was measured in the experimental setup described in Section 3.1 and followed the same analysis procedure as in case of  $\text{CaMoO}_4$  crystals. The results of the measurements are summarized in Table 4. In general, annealing at  $800\text{ }^\circ\text{C}$  for 48 hours in oxygen flow substantially improved RLY of the  $\text{ZnWO}_4$  crystals. This increase can be explained by the deficit of oxygen content in the delivered crystals which was compensated by the annealing in oxygen flow<sup>6</sup>. Figure 5 shows  $^{137}\text{Cs}$  spectra measured with  $\text{ZnWO}_4$ -4 crystal before and after annealing by PMT at room temperature (see Section 3.1). From this figure it is evident that the decomposition into two Gaussians gives a much better fit to a measurement than the fit to a single Gaussian as would be expected. This effect can be partially explained with geomet-

<sup>6</sup> The emission of the luminescence light is associated with the radiative transition between tungsten and oxygen within the  $(\text{WO}_6)^{6-}$  molecular complex.

Table 3

Upper limits on the activities of the  $\text{ZnWO}_4$ -3 crystal (=40 mm, height=16 mm, mass=163 g) for the different isotopes from the  $^{232}\text{Th}$ -, the  $^{238}\text{U}$ - and the  $^{235}\text{U}$ -decay chain, as well as for  $^{40}\text{K}$ . When several  $\gamma$  lines were used for the calculation of the activity of one isotope, the quoted value is the weighted average of the single activities. The limits given for the whole decay chain are again the weighted averages of the activities of the single isotopes [24].

Isotope	Activity (90%C. L.)
K-40	$<321.3^{+29.8}_{-26.2}$ mBq/kg
$^{228}\text{Ac}$	$<124.6^{+8.0}_{-7.1}$ mBq/kg
$^{212}\text{Pb}$	$<315.7^{+50.7}_{-47.2}$ mBq/kg
$^{212}\text{Bi}$	$<266.5^{+18.3}_{-16.0}$ mBq/kg
Th-232 chain	$<151.1^{+7.3}_{-6.5}$ mBq/kg
$^{234}\text{Pa}$	$<562.3^{+52.0}_{-45.7}$ mBq/kg
$^{226}\text{Ra}$	$<29.9^{+2.8}_{-2.5}$ Bq/kg
$^{214}\text{Pb}$	$<115.4^{+8.7}_{-7.7}$ mBq/kg
$^{214}\text{Bi}$	$<159.4^{+10.5}_{-9.3}$ mBq/kg
U-238 chain	$<140.5^{+6.6}_{-5.9}$ mBq/kg
$^{235}\text{U}$	$<3.61^{+0.33}_{-0.29}$ Bq/kg
$^{227}\text{Th}$	$<1.20^{+0.25}_{-0.24}$ Bq/kg
$^{211}\text{Pb}$	$<161.5^{+16.7}_{-15.9}$ mBq/kg
U-235 chain	$<175.7^{+16.7}_{-15.9}$ mBq/kg

Table 4

Relative light yield of  $\text{ZnWO}_4$  crystals measured at room temperature with a PMT. The light yield of each  $\text{ZnWO}_4$  crystal with applied spectral correction was normalized to the light yield of our standard  $\text{CaWO}_4$  crystal (see text for details).

	RLY (%)	Resolution (%) at 662 keV
<b><math>\text{ZnWO}_4</math>-1 (=40 mm, height=10 mm, mass=92.5 g)</b>		
as arrived	95.4	19.3
annealing 1 at 800°C for 24h	101	16.7
roughened after annealing 1	117	10.8
annealing 2 at 900°C for 48h, roughened	107	10.8
<b><math>\text{ZnWO}_4</math>-3 (=40 mm, height=16 mm, mass=163 g, roughened)</b>		
as arrived	118	12.5
<b><math>\text{ZnWO}_4</math>-4 (=40 mm, height=40 mm, mass=404.4 g, roughened)</b>		
as arrived	83.6	15.7
annealed at 800°C for 48h	111.1	16

rical trapping of scintillation light due to the total internal reflections at the crystal surfaces [17]. Probably because of the increased transparency of the crystal (which has an impact on the light propagation through the crystal) a double

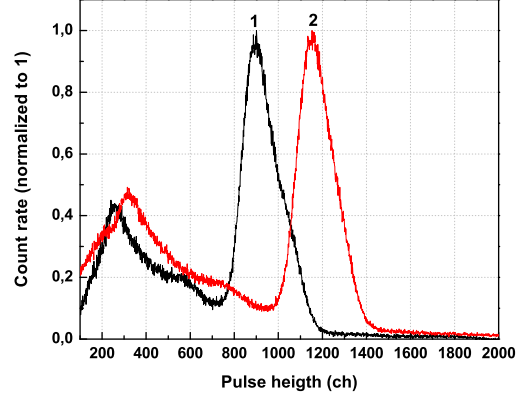


Fig. 5.  $^{137}\text{Cs}$  spectra measured with the roughened  $\text{ZnWO}_4$ -4 crystal before annealing (1) and after annealing at 800 °C for 48 hours in oxygen flow (2). Measurements were performed at room temperature with a PMT (see text for details).

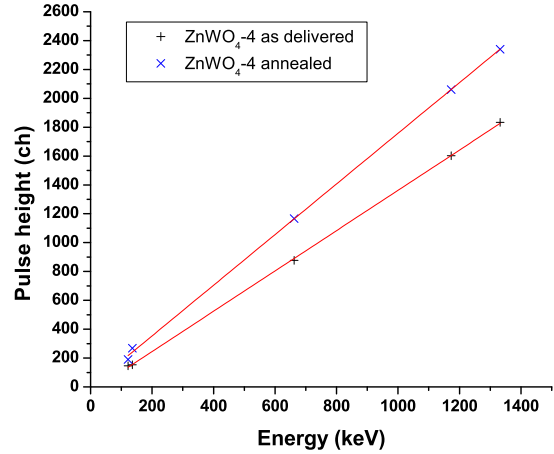


Fig. 6. Linearity of the scintillation response of the  $\text{ZnWO}_4$ -4 crystal before and after annealing at 800 °C for 48 hours in oxygen flow. Measurements were taken via irradiation of the crystal with  $\gamma$ 's from  $^{57}\text{Co}$  (122 keV and 136 keV),  $^{137}\text{Cs}$  (662 keV) and  $^{60}\text{Co}$  (1.17 MeV and 1.33 MeV) calibration sources. Measurements were performed at room temperature with a PMT (see text for details).

structure of the  $^{137}\text{Cs}$  photopeak almost disappeared after applying the annealing procedure. Further investigations of the influence of annealing on the scintillation properties of  $\text{ZnWO}_4$  crystals are in progress.

Roughening of the flat surface of the crystal with boron carbide powder further improved the RLY and energy resolution, thus additionally reducing trapping of the scintillation light within the crystal.

A good linearity of the scintillation response between 122 keV and 1.33 MeV was measured with the  $\text{ZnWO}_4$ -4 crystal before and after annealing, see Fig. 6.

Table 5

Gluing of different thermometer carriers on a  $\text{ZnWO}_4$  crystal. After cooling to mK temperatures, surface quality of some crystals remained unchanged (-), whereas degradation was observed for others (+), see text for details.

	CaWO <sub>4</sub> wafer (20×10×1) mm <sup>3</sup>	ZnWO <sub>4</sub> wafer (20×10×1) mm <sup>3</sup>
Epo-Tek 301-2	-	-
Araldite 2011	+	+

#### 4.2. W-SPT on $\text{ZnWO}_4$ crystals

The research performed in [25] has shown that very high deposition temperatures of  $\sim 740$  °C are needed in order to obtain transition temperatures of  $\sim 22$  mK for W-SPT on  $\text{ZnWO}_4$  crystals. Heating up a crystal to such a high temperature in vacuum degrades the scintillation output of a crystal dramatically. Therefore, we decided to grow a W-SPT on a separate thermometer carrier and to apply a novel gluing technique [26,27] to produce a phonon detector based on a  $\text{ZnWO}_4$  crystal (see Section 4.3).

A  $(20 \times 10 \times 1)$  mm<sup>3</sup>  $\text{ZnWO}_4$  wafer of known orientation was mounted into the tungsten deposition system and slowly heated up to 600 °C in vacuum, and kept at this temperature during the whole deposition process. To prevent inter-diffusion between the tungsten film and the  $\text{ZnWO}_4$  crystal surface we first deposited a 2 k layer of  $\text{SiO}_2$ . Then, a 2 k layer of tungsten was evaporated. The  $\sim 120$  mΩ resistance of the W-SPT on the  $\text{ZnWO}_4$  wafer was measured as described in Section 3.2 while applying 50 nA bias current. Transition temperatures as low as  $\sim 19$  mK were achieved using the deposition procedure described above. The characteristics of the obtained transition curve fulfill the quality requirements of the W-SPT for the CRESST-II phonon detectors.

#### 4.3. $\text{ZnWO}_4$ phonon detector with a separate thermometer carrier

Since  $\text{ZnWO}_4$  crystals tend to easily cleave along the (010) plane, we first investigated the influence of the glue layer on the surface properties of the crystals. Two different glues, namely Araldite 2011 and Epo-Tek 301-2<sup>7</sup>, and two different thermometer carrier crystals ( $\text{CaWO}_4$  and  $\text{ZnWO}_4$ ) were tested. In each test, the carrier crystal was glued with a certain glue type on a  $\text{ZnWO}_4$  crystal (=40 mm, height=10 mm). This composite structure was then mounted in a copper holder and cooled down to mK temperatures. The results of these measurements are summarized in Table 5. Only in case of gluing with Epo-Tek 301-2 surface quality of crystals remained unchanged,

<sup>7</sup> Araldite 2011 is a registered trademark of the Huntsman Corporation. Epo-Tek 301-2 is a registered trademark of the Epoxy Technology.

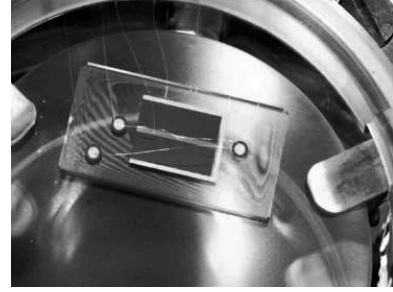


Fig. 7.  $\text{ZnWO}_4$  phonon detector with the separate  $\text{ZnWO}_4$  thermometer carrier mounted in a copper holder. The crystal is held by six pairs of bronze clamps coated with an Al layer and with an Araldite 2011 scintillating layer. The whole structure is surrounded by a highly reflecting foil VM2002. The bond wires for the electrical contacts are visible.

whereas degradation was observed in case of gluing with Araldite 2011.

The  $(20 \times 10 \times 1)$  mm<sup>3</sup>  $\text{ZnWO}_4$  wafer of known orientation (plane (010) is perpendicular to the  $(20 \times 10)$  mm<sup>2</sup> surface of the wafer) with the W-SPT on it (see Section 4.2) was glued with Epo-Tek 301-2 on the  $\text{ZnWO}_4$ -4 target crystal of known orientation (plane (010) is perpendicular to the flat surface of the crystal). Figure 7 shows the produced  $\text{ZnWO}_4$  phonon detector with the glued thermometer carrier mounted in a copper holder.

## 5. Conclusions

In the framework of the CRESST-II experiment we developed reliable techniques for the production of cryogenic phonon detectors based on  $\text{CaMoO}_4$  and  $\text{ZnWO}_4$  scintillating crystals. The light output of  $\text{CaMoO}_4$  and  $\text{ZnWO}_4$  crystals at room temperature have been studied. Furthermore, the influence of the mechanical (polishing, roughening) and thermal treatment (annealing, W-SPT deposition) on the light output of these scintillating crystals has been investigated.

The developed prototype  $\text{ZnWO}_4$  phonon detector with a separate glued on thermometer was installed into the main CRESST-II experimental setup at Gran Sasso underground laboratory for the ongoing dark matter Run 31 and has already shown promising results. The scintillation response of the  $\text{CaMoO}_4$  crystals at low temperatures is the subject of the ongoing investigation.

## References

- [1] F. Zwicky *Helv. Phys. Acta* 6 (1933), 110-127.
- [2] G. Jungman et al. *Phys. Rep.* 267 (1996), 195-373.
- [3] J. A. R. Caldwell et al. *Ap. J.* 251 (1981), 61.
- [4] G. Angloher et al. to be published (2008); arXiv: 0809.1829
- [5] B. Majorovits et al. *Rev. Sci. Instr.* 78 (2007), 073301.
- [6] G. Angloher et al. *Astropart. Phys.* 18 (2002), 43-55.
- [7] G. Angloher et al. *Astropart. Phys.* 23 (2005), 325-339.
- [8] P. Meunier et al. *Appl. Phys. Lett* 75 (1999), 1335.

- [9] M. Korzhik et al. IEEE Trans. Nucl. Sc. 55 (2008), 1473.
- [10] P. Lecoq et al, *Inorganic scintillators for detector systems (physical principles and crystal engineering)*, printed by Springer-Verlag Berlin Heidelberg (2006), p. 21.
- [11] K. Schäfner Max Planck Institute for Physics private communication (2008).
- [12] F. Petricca et al. Nucl. Instr. Meth. A520 (2004), 193-196.
- [13] R. F. Lang Max Planck Institute for Physics private communication (2008).
- [14] V. B. Mikhailik et al. Nucl. Instr. Meth. A583 (2007), 350-355.
- [15] A. N. Annenkov et al. Nucl. Instr. Meth. A584 (2008), 334-345.
- [16] S. Pirro et al. Phys. Atom. Nucl. 69 (2006), 2109-2116.
- [17] J. Ninkovich PhD thesis Technische Universität München (2005) 55;  
<http://publications.mppmu.mpg.de/2005/MPP-2005-16/FullText.pdf>
- [18] R. K. Swank et al. Rev. Sci. Inst. 29 (1958), 279-284.
- [19] F. Pröbst et al. J. Low Temp. Phys. 100 (1995), 69.
- [20] F. Pröbst Max Planck Institute for Physics private communication (2007).
- [21] I. Bavykina et al. IEEE Trans. Nucl. Sc. 55 (2008), 1449.
- [22] H. Kraus et al. Phys. Lett. B610, issues 1-2 (2005), 37-44.
- [23] Ya. V. Vasiliev et al. J. Cryst. Growth 229 (2001), 305-311.
- [24] M. Hofmann E15 group Technische Universität München private communication (2008).
- [25] I. Bavykina Diploma thesis Universität Siegen (2006), p. 52;  
<http://publications.mppmu.mpg.de/2006/MPP-2006-114/FullText.pdf>
- [26] M. Kiefer et al. to be published in Optical Materials (2008).
- [27] J.-C. Lanfranchi PhD thesis Technische Universität München (2005), p. 55.